OXFORD

Cerebral Cortex, 2023, **33**, 2788–2803
https://doi.org/10.1093/cercor/bhac242
Advance access publication date 25 June 2022
Original Article

Maturation of large-scale brain systems over the first month of life

Ashley N. Nielsen[1,*], Sydney Kaplan[1], Dominique Meyer[1], Dimitrios Alexopoulos[1], Jeanette K. Kenley[1], Tara A. Smyser[2], Lauren S. Wakschlag[3,4,5], Elizabeth S. Norton[3,4,6], Nandini Raghuraman[7], Barbara B. Warner[8], Joshua S. Shimony[9], Joan L. Luby[2], Jeffery J. Neil[1,9], Steven E. Petersen[1], Deanna M. Barch[2,9,10], Cynthia E. Rogers[6,9], Chad M. Sylvester[2], Christopher D. Smyser[1,8,9]

[1]Department of Neurology, Washington University in St. Louis, 660 S. Euclid Ave, St. Louis, MO, 63110, USA,
[2]Department of Psychiatry, Washington University in St. Louis, 660 S. Euclid Ave, St. Louis, MO, 63110, USA,
[3]Institute for Innovations and Developmental Sciences, Northwestern University, 420 E Superior, Chicago, IL, 60611, USA,
[4]Department of Medical Social Sciences, Northwestern University, 420 E Superior, Chicago, IL, 60611, USA,
[5]Feinberg School of Medicine, Northwestern University, 420 E Superior, Chicago, IL, 60611, USA,
[6]Department of Communication Sciences and Disorders, Northwestern University, 420 E Superior, Chicago, IL, 60611, USA,
[7]Department of Obstetrics and Gynecology, Washington University in St. Louis, 660 S. Euclid Ave, St. Louis, MO, 63110, USA,
[8]Department of Pediatrics, Washington University in St. Louis, 660 S. Euclid Ave, St. Louis, MO, 63110, USA,
[9]Department of Radiology, Washington University in St. Louis, 660 S. Euclid Ave, St. Louis, MO, 63110, USA,
[10]Department of Psychological and Brain Sciences, Washington University in St. Louis, 660 S. Euclid Ave, St. Louis, MO, 63110, USA
*Corresponding author: 660 S. Euclid, Campus Box 8511, St. Louis, MO, 63110, United States. Email: ashley.nielsen@wustl.edu

The period immediately after birth is a critical developmental window, capturing rapid maturation of brain structure and a child's earliest experiences. Large-scale brain systems are present at delivery, but how these brain systems mature during this narrow window (i.e. first weeks of life) marked by heightened neuroplasticity remains uncharted. Using multivariate pattern classification techniques and functional connectivity magnetic resonance imaging, we detected robust differences in brain systems related to age in newborns ($n = 262$; $R^2 = 0.51$). Development over the first month of life occurred brain-wide, but differed and was more pronounced in brain systems previously characterized as developing early (i.e. sensorimotor networks) than in those characterized as developing late (i.e. association networks). The cingulo-opercular network was the only exception to this organizing principle, illuminating its early role in brain development. This study represents a step towards a normative brain "growth curve" that could be used to identify atypical brain maturation in infancy.

Key words: infant; functional connectivity; fMRI; machine learning; development.

Introduction

The period immediately after birth is a critical window when the foundational elements of the brain's functional and structural architecture are established and early postnatal experience can begin to influence ongoing brain development. During this period, a number of complex, interrelated neurobiological processes (e.g. myelination, axonal pruning, synaptogenesis, synaptic pruning, changes in ion channel function, and changes in gene expression) unfold in an ordered manner both across the brain and over time (Sydnor et al. 2021). A considerable amount of reconfiguration and reorganization (e.g. retraction of 70% of callosal fibers in primates; LaMantia and Rakic 1990) occurs during this period as a normative response to the environment (e.g. sensory exposure in the hospital after birth relates to brain morphometry and later language outcomes; Pineda et al. 2014). Deleterious experiences in early life including sensory deprivation (Knudsen 2004), neglect (Bick and Nelson 2015), stress (Avishai-Eliner et al. 2002; Chen and Baram 2015), and trauma (Thomason and Marusak 2017) disrupt these key developmental processes, producing long-lasting consequences on brain structure and function. Furthermore, developmental disorders and developmental psychopathology are now increasingly recognized to have their origins in infancy, with symptomatic presentation occurring during childhood and beyond as a result of the cascading effects of atypical early brain development (Monk et al. 2019; Wakschlag et al. 2019). Though the importance of this window for human brain development is irrefutable, long-standing investigations of the developmental processes occurring during infancy have yet to delineate the patterns of change across large-scale brain systems over the first weeks of life.

Investigating early brain development at the level of large-scale brain systems can provide innovative insights into the coordinated developmental mechanisms occurring up to and during infancy. For example, synaptogenesis (Huttenlocher and Dabholkar 1997), dendritic growth and arborization (Travis et al. 2005), the myelination, growth, and functional specialization

Received: January 20, 2022. **Revised:** April 29, 2022. **Accepted:** May 23, 2022

of thalamocortical connections (Flechsig Of Leipsic 1901; Toulmin et al. 2015), the myelination of intra-cortical connections (Miller et al. 2012), cortical expansion (Hill et al. 2010), and the refinement of cortical microstructure (Smyser et al. 2016b; Natu et al. 2021) occur at different rates across the brain, largely in line with the boundaries of large-scale brain systems. During the prenatal period, there is rapid growth and refinement of thalamo-cortical fibers such that primary sensorimotor cortex appears more refined than that of heteromodal cortex (Huttenlocher and Dabholkar 1997; Travis et al. 2005). Over the course of development from infancy to adulthood, brain systems important for sensorimotor function (e.g. somatosensory, motor, visual, and auditory) generally mature earlier than those important for higher-order cognition (e.g. default mode, executive control, and attention networks) such that sensorimotor and association brain systems have been categorized as "early developing" and "late developing," respectively (Sydnor et al. 2021). Although these neurodevelopmental processes occur over the course of years for later developing brain systems (e.g. myelination of executive control networks into early adulthood (Lebel et al. 2019)), differential rates of development are apparent early in life (Flechsig Of Leipsic 1901; Huttenlocher and Dabholkar 1997; Travis et al. 2005; Hill et al. 2010; Miller et al. 2012; Toulmin et al. 2015; Smyser et al. 2016b; Natu et al. 2021). However, it is not clear whether the large-scale organization of the brain constrains the neurodevelopmental processes occurring during the neonatal period. Brain activity across large-scale brain systems has also been shown to be coordinated at rest (i.e. functional networks) using functional connectivity magnetic resonance imaging (fc-MRI; Biswal et al. 1995; Power et al. 2011). Because this coordinated brain activity is sensitive to changed brain structure (Gratton et al. 2012; Warren et al. 2014) and experience-dependent change (Newbold et al. 2020, 2021), examining developmental change in the functional connectivity (FC) of brain systems during infancy provides a window into the interrelated structural and functional neurobiological processes that contribute to maturing brain function.

The development of large-scale brain systems has been well-characterized through late childhood and adolescence using FC (Marek et al. 2015, 2019; Nielsen et al. 2019), but has not been fully described in infancy. Precursors of mature functional networks have been observed during gestation (Turk et al. 2019) and at birth in premature (Smyser et al. 2011; Duerden et al. 2013) and full-term born infants (Fransson et al. 2007; Gao et al. 2009; Doria et al. 2010; Gao et al. 2015; Eyre et al. 2021), but most studies have examined developmental differences in FC over relatively long periods of time (e.g. infancy to adulthood). The relative maturity of infant functional networks appears consistent with the proposed framework of "early" vs. "late" developing systems; functional connectivity of sensorimotor networks appears more mature than that of association networks in infancy (Doria et al., 2010; Eyre et al., 2021; Fransson et al., 2007; Gao et al., 2009, 2015; Lin et al., 2008; Smyser et al., 2010). However, this work has not examined how FC varies on a shorter timescale (i.e. first 4 weeks of life). Specifically identifying and characterizing how functional networks vary according to postmenstrual age (PMA) during this critical window is a necessary step for identifying variation related to atypical development, an infant's environment, and/or a clinical intervention.

The goal of this study was to noninvasively characterize, using fc-MRI, the development of large-scale brain systems during the neonatal period. Multivariate pattern classification methods were applied to a large sample of healthy, full-term infants ($n = 262$; PMA: mean = 41.8; std = 1.25; range = 38–45 weeks) and an independently collected validation sample ($n = 50$; PMA: mean = 41.8; std = 1.66; range = 38–45 weeks) to robustly detect evidence of developmental change in FC over the first month of life. Then, each individual functional network was evaluated to reveal whether the observed developmental differences in FC during the neonatal period reflected differential development across brain systems. Whether the development of FC from sensorimotor and association networks differed during the neonatal period was specifically tested, given the evidence distinguishing these "early" and "late" developing brain systems (Sydnor et al. 2021). Our findings contribute to an improved understanding of normative brain development in early life and could be used to better target the long-lasting consequences of atypical brain maturation in infancy due to heritable disorders and/or adverse early life experiences.

Methods and materials

Participants

eLABE sample

This study was approved by the Human Studies Committees at Washington University in St. Louis and informed consent was obtained from a parent of all participants. Neonates were recruited as a part of the Early Life Adversity, Biological Embedding, and Risk for Developmental Precursors of Mental Health Disorders (eLABE) cohort, whose participants were recruited under the parent March of Dimes study (Stout et al. 2021). Pregnant mothers were recruited and enrolled between the second and third trimesters. Recruitment oversampled mother–infant pairs facing adversity (e.g. poverty and stress). The study includes neonatal magnetic resonance imaging (MRI) performed shortly after birth. Inclusion criteria for the study included speaking English, mother age 18 years or older, and singleton birth. Excluded were women with alcohol or other substance abuse (cannabis use was not excluded). Anatomic MR images were reviewed by a neuroradiologist (J.S.S.) and pediatric neurologist (C.D.S.). Subjects were excluded from the current analyses if they had evidence of brain injury or were born preterm (<37 weeks gestational age, GA). Additional exclusion

criteria included pregnancy complications (but not gestational diabetes or hypertension) and known fetal abnormalities including intrauterine growth restriction. A maternal medical risk (MMR) score was calculated for each participant using survey data and medical chart review (Bateman et al. 2013). Of the 385 participants who were scanned for eLABE, 262 were included in the current analyses. Subjects were excluded for the following reasons: no functional magnetic resonance imaging (fMRI) data collected ($n = 3$), no usable T2 for registration ($n = 28$), <37 weeks GA at birth ($n = 52$), brain injury ($n = 17$), required intubation or chest tube ($n = 4$), neonatal intensive care unit stay for > 7 days ($n = 30$), and birthweight < 2,000 g ($n = 1$). There were 279 neonates who did not meet any of these exclusion criteria (note that some met multiple exclusion criteria). An additional 8 neonates were excluded because they did not have ≥10 min of usable fMRI data after motion censoring (see below), and 9 were excluded based on visible artifacts in FC data, resulting in 262 subjects in the current dataset.

Validation sample

The following 2 separate studies contributed to the validation sample ($n = 50$).

CUDDEL. This study was approved by the Human Studies Committees at Washington University in St. Louis, and informed consent was obtained from a parent of all participants. Neonatal participants were recruited as a part of the parent study Prenatal Cannabis Use (PCU) and Development of Offspring Brain and Behavior During Early Life (0–18 months) (CUDDEL). Pregnant mothers were recruited and enrolled between the second and third trimesters. The current study focused on neonatal MRI performed shortly after birth. Inclusion criteria for the current study included speaking English, mother age 18 years or older, cannabis use at least once during the subject's lifetime, and full-term singleton birth (≥37 weeks GA at birth). Excluded were women with alcohol or other substance abuse (cannabis use was not excluded). Both cases (infants born to women that indicated PCU) and controls (infants born to women that indicated no PCU) were included. Anatomic MR images were reviewed by a neuroradiologist (J.S.S.) and pediatric neurologist (C.D.S.). Collection of MRI data for this study is ongoing. Of the 46 participants that have been scanned for CUDDEL, 45 were included in the current analyses. One subject was excluded for brain injury.

O2P2. This study was approved by the Human Studies Committees at Washington University in St. Louis, and informed consent was obtained from a parent of all participants. Neonatal participants were recruited as a part of the parent Oxygen Part 2 (O2P2) study. Mothers were recruited during their postpartum stay. The current study focused on neonatal MRI performed within 72 h of delivery. Inclusion criteria for the current study included full-term singleton birth, English speaking, and Covid-19 negative result within the last 5 days. Exclusion criteria were major fetal anomaly, multiple gestation, category III electronic fetal monitoring, maternal hypoxia, umbilical artery Doppler abnormalities, preeclampsia, intrauterine growth restriction, pregestational diabetes, current tobacco smoker, Covid-19 positive, or declined Covid-19 testing. After delivery, all infants were admitted to the Newborn Nursery and were not be admitted to the NICU. Anatomic MR images were reviewed by a neuroradiologist (J.S.S.) and pediatric neurologist (C.D.S.). Collection of MRI data for this study is ongoing. Of the 5 participants that have been scanned for O2P2, 5 were included in the current analyses.

Estimation of PMA at Scan

PMA at scan was calculated by combining the completed weeks of gestation at delivery (GA at birth) with the weeks between birth and scan (chronological age at scan). GA at birth was acquired through medical records upon enrollment in the eLABE, CUDDEL, or O2P2 studies and was determined by best obstetric estimate including last menstrual period or earliest ultrasound dating available (Stout et al. 2021). Because due dates can imprecisely measure the time between conception and birth, in this study GA at birth was quantified using only the completed weeks of gestation.

Image acquisition

Both the eLABE and validation samples were imaged using the same procedures and same MRI sequences. After feeding, the infant was swaddled and positioned in a head-stabilizing vacuum fix wrap. A nurse familiar with neonate transport and resuscitation was present at all MRI scans. Heart rate and blood oxygenation were measured continuously throughout all scans, and infants were monitored visually via video. Based on visual monitoring through a camera, infants slept through scans as indicated by eye closure and minimal movements. Imaging was performed without sedating medications using a Siemens 3T Prisma scanner and 64-channel head coil. A T2-weighted image (sagittal, 208 slices, 0.8-mm isotropic resolution, time echo, TE = 563 ms, time repetition, TR = 4,500/3,200 ms for eLABE) was collected. For the resting-state fMRI, functional imaging was performed using a blood-oxygen-level dependent (BOLD) gradient-recalled echo-planar multiband (MB) sequence (72 slices, 2.0-mm isotropic resolution, TE = 37 ms, TR = 800 ms, MB factor = 8). Spin-echo field maps were obtained (at least 1 anterior–posterior and 1 posterior–anterior) during each session with the same parameters. Between 2 and 9 fMRI BOLD scans were acquired, depending on how the infant tolerated the scan (mean 3.75 runs). Scans were collected in both the anterior–posterior (AP) and posterior–anterior (PA) direction; a typical scan session included 2 AP runs and 2 PA runs. The scans were 420 frames, which is 5.6 min in length.

Image preprocessing and FC processing

Both the eLABE and validation samples were processed in an identical manner to limit potential differences due

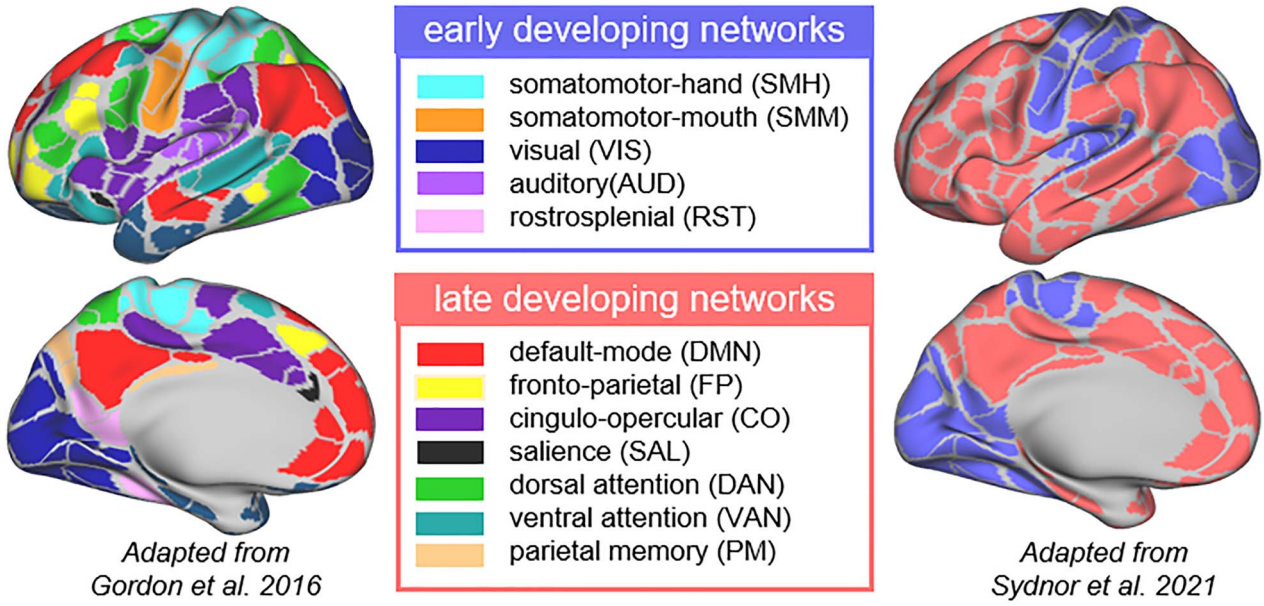

Fig. 1. Parcellation and functional network definitions used to quantify FC and to group functionally related regions in the neonatal brain. The 333 parcels and 12 functional networks were previously defined in healthy adults in Gordon et al. (2016). Analyses were also conducted with 2 separate parcellation schemes (Supplement 1) to ensure that results were not dependent on this parcellation. Parcels and functional networks were also grouped as either early (light blue) or late (light red) developing according to a review of previous studies of the developmental trajectories of these brain systems from infancy to adulthood (Sydnor et al. 2021).

to analysis across cohorts, incorporating surface-based strategies to account for individual and developmental differences in cortical folding. fMRI preprocessing included correction of intensity differences attributable to interleaved acquisition, bias field correction, intensity normalization of each run to a whole-brain mode value of 1,000, linear realignment within and across runs to compensate for rigid body motion, and linear registration of BOLD images to the adult Talairach isotropic atlas. Neonates were registered: BOLD to individual T2 to group-average T2 from this cohort to 711-2N Talairach atlas. Field distortion correction was performed, using the FSL TOPUP toolbox (http://fsl.fmrib.ox.ac.uk/fsl/fslwiki/TOPUP).

Following initial processing, the surface-based neonatal parcellation approach, Melbourne Children's Regional Brain Atlases (MCRIB), was used to generate surfaces for each subject and the volumetric resting-state BOLD timeseries were mapped to subject-specific surfaces using established procedures adapted from the Human Connectome Project as implemented in Connectome Workbench 1.2.3.

After mapping to the surface, each dataset underwent rs–fc preprocessing. In the initial iteration, the data were processed with the following steps: (i) demean and detrend within run, (ii) multiple regression with nuisance timeseries including white matter, ventricles, extra-axial cerebrospinal fluid, and whole brain, as well as 24-parameter Friston expansion regressors derived from head motion. Next, frames contaminated by motion were censored as described below. Finally, the initial rs–fc preprocessing stream was repeated on the output of the initial preprocessing using only the frames that had passed motion criteria, with the addition of interpolating censored frames and band-pass filtering ($0.009\ \text{Hz} < f < 0.08$ for children).

fMRI data were censored at FD > 0.25 mm, with the additional restriction that only epochs of at least 3 consecutive frames FD < 0.25 mm were included. This FD threshold was selected after taking into account the smaller radius of infants' heads (Smyser et al. 2010) and reviewing motion traces in several subjects (Power et al. 2012; Power et al. 2014). In order to be included in the study, a minimum of 10 min (750 frames) of data were required. To test for any potential patterns of FC related to head motion or amount of data, we calculated (i) the number of frames retained after censoring, (ii) the % of frames retained after censoring, (iii) the average FD across all frames (precensoring), and (iv) the average FD across all frames with FD < 0.25 mm for each individual subject. The impact of different motion de-noising strategies on age prediction and head motion prediction with FC was also examined (Supplement 2).

fMRI data were aligned across subjects into the "fs_LR32k" surface space using spherical registration. Timecourses for surface data were smoothed with geodesic 2D Gaussian kernels ($\sigma = 2.25$ mm). To test for potential patterns of FC related to brain size or cortical folding, we calculated (i) total brain volume (i.e. volume of the number of voxels that are neither background, extra-axial centrospinal fluid, ventricles, nor brain stem), (ii) intracranial volume (i.e. volume of the number of voxels inside the skull), and (iii) gyrification index (i.e. the ratio of the area of the mid-thickness cortical surface to the surface area of the cerebral hull (Shimony et al. 2016; van Essen 2005)).

Functional connectivity network construction

For each participant, whole-brain FC was generated by extracting the timeseries from 333 previously-defined surface parcels (Gordon et al. 2016, Fig. 1) and calculating the Fisher z-transformed Pearson correlation between each pair of parcels. For each individual, this yields a 333 × 333 correlation matrix. Because there is not yet consensus on the spatial layout of neonatal functional networks (Lin et al. 2008; Gao et al. 2009; Doria et al. 2010; Gao et al. 2015; Eyre et al. 2021), we used definitions of functional networks derived in healthy adults (Gordon et al. 2016). Functional networks include processing networks like the auditory (AUD), visual (VIS), somatomotor-hand (SMH), somatomotor-mouth (SMM), retrosplenial (RST), and control and other association networks like the frontoparietal (FP), cingulo-opercular (CO), dorsal attention (DAN), ventral attention (VAN), salience (SAL), default mode (DMN), and parietal memory (PM). We also generated whole-brain FC using 400 and 1,000 previously-defined cortical parcels (Schaefer et al. 2018) to examine the potential role of parcellation on subsequent analyses and results (Supplement 1).

Multivariate machine learning procedures

Support vector regression (SVR) with a linear kernel was implemented to identify multivariate patterns of FC that carry information about PMA at scan (Dosenbach et al. 2010; Nielsen et al. 2019). This approach was chosen because infant brain development is complex and comprised of several developmental processes that occur across many brain systems (Sydnor et al. 2021) and because these methods have been previously used to detect differences in brain maturity from FC in infancy (Smyser et al. 2016b) and later in development (Dosenbach et al. 2010; Satterthwaite et al. 2013; Nielsen et al. 2019). SVR is a sensitive and powerful tool to extract the multivariate relationship between a set of many features (here, functional connections) and labels (here, PMA at scan) in a training sample, which can subsequently be applied to make predictions about unseen test individuals. Ten-fold cross-validation was used to identify patterns of FC in the training set (i.e. 90% of the eLABE sample) and test whether these patterns could accurately discriminate differences in maturity in the remaining individuals in the test set (i.e. 10% of the eLABE sample). Ten-fold cross-validation was repeated with 100 random partitions of the dataset into training and test sets to ensure that performance was not due to serendipitous random seeding (Supplementary Fig. S3).

Age prediction in the eLABE sample and the validation sample

First, all 55,278 functional connections among the 333 parcels were included as features and within-sample age prediction was evaluated through 10-fold cross-validation. Predictive approaches like SVR are designed to optimize prediction and could potentially identify multivariate patterns of FC that do not generalize to describe early brain development outside of the original training sample (Nielsen et al. 2020b). Cross-validation alone is not a sufficient test of the robustness of data-driven, multivariate predictive models (Varoquaux et al. 2017). For each fold of cross-validation, the identified multivariate patterns of FC were also applied to predict the PMA at scan of the individuals in the validation sample. This generates a single predicted PMA at scan based on FC for each individual in the eLABE sample and 10 predicted PMA at scan (i.e. for each fold of 10-fold cross-validation) for each individual in the validation sample. Performance was quantified by calculating the correlation between the predicted PMA and actual PMA (i.e. R^2) in the eLABE and validation samples separately. We then tested whether the predicted PMA based on FC was significantly more accurate than expected by chance. We used SVR to extract the multivariate relationship between FC and randomly permuted PMA at scan in the eLABE sample, a null age prediction model ($n = 100$). Age prediction performance was then compared to age prediction with the null models. Mean squared error (MSE) was also calculated to evaluate age prediction from FC in both the eLABE and validation samples.

Age prediction in relation to other covariates

The extent to which other variables potentially related to PMA at scan (e.g. head motion and brain morphometry) contributed to the observed age prediction with FC was examined. Two approaches were employed to measure the impact of the following variables: (i) precensoring mean FD, (ii) postcensoring mean FD, (iii) amount of data, (iv) head size (i.e. intracranial volume), and (v) cortical folding (gyrification index). First, SVR was used to determine the extent to which multivariate patterns of FC carried information about these other covariates (Supplement 2). Second, these covariates were regressed from the FC and from PMA at scan before age prediction and the impact on performance were examined. Within each fold of 10-fold cross-validation, linear models were fit to capture the relationship between the regressors and the FC from each functional connection (55,278) and the relationship between the regressors and PMA at scan, separately in the training set and testing set. The residuals from these models were then used as the features and labels for training and testing with SVR. The same strategy was used in the independent validation sample. We examined the separate impact of data quality regressors (motion and amount of data) and biological regressors (intracranial volume and cortical folding) as well as each individual regressor alone (Supplement 2).

Age prediction with FC from individual functional networks

Second, only the FC from a single functional network was used for age prediction. Feature selection (i.e. restricting the number of features used for training) was used to test the extent to which the FC from a single network might capture the variance in FC related to age during

the neonatal period. For each network, all connections associated with parcels from a single functional network (e.g. within the CO and between the CO and the rest of the brain, Supplementary Fig. S1) were sub-selected and then only those features were used for age prediction. Because age prediction with FC can depend on how many features are used (Nielsen et al. 2019, 2020b), for each network a matched set of functional connections randomly selected from the matrix was also generated and then these randomly selected features were used for age prediction. Fifty matched randomly selected feature sets were generated for each network. The same number of connections as in a single functional network was randomly selected from multiple functional networks. Age prediction with features from a single network was then compared to age prediction with these matched randomly selected features.

To further disentangle the relationship between age prediction, network size, and network identity, age prediction when the same number of features from the same number of parcels were selected from each functional network was compared. A number of parcels from a single functional network was randomly sub-selected, from a single parcel to the maximum number of parcels in a network (e.g. for DMN = 41). Only the FC from the connections associated with those sampled parcels was then used as features for age prediction (number of features: 333–13,653). This process was repeated 50 times for each network and each parcel number. The average age prediction as a function of sampled parcel number was generated for each functional network.

Lastly, we compared age prediction when FC was sampled from early developing vs. late developing functional networks. A set number of parcels (10, 20, 30, 40, and 50) were randomly sub-selected from either early developing networks (SMH, SMM, AUD, VIS, and RST) or late developing networks (CO, FP, VAN, DAN, SAL, and DMN). Only the FC from the connections with those sampled parcels was then used as features for age prediction (number of features: 3,330–16,650). This process was repeated 50 times for the early and late networks and for each parcel number. The null was generated by randomly sampling from the entire set of parcels and using the sub-selected FC for age prediction. Differences in age prediction were statistically evaluated using the Steiger's paired *t*-statistic, which tests the null hypothesis that 2 variables (i.e. predicted PMA at scan using FC from early or late networks) are equally linearly correlated with a third variable (i.e. true PMA at scan; Steiger 1980). Steiger's *t*-statistics were used to compare age prediction when using FC from parcels that were sampled from early developing networks, late developing networks, or randomly from the entire set.

Age prediction with permuted FC from individual networks, blocks, or parcels

Feature permutation (i.e. manipulating a restricted set of features used for testing) was used to investigate whether a given set of features was necessary to capture the brain-wide patterns of FC that facilitate age prediction. Permutation sensitivity analysis disrupts the true relationship between age and FC present in a limited set of features by permuting these features across the subjects in the test set (see Supplementary Fig. S2). The model trained to predict age using all the features is then applied to the test set containing permuted features. Permuting these features will negatively impact age prediction with brain-wide FC if a set of features is uniquely important for age prediction. For each tested set of features, the impact of 50 different permutations of subject order in the test set for each fold of cross-validation was averaged. This approach was applied at the network, block, and parcel level as described below.

Networks

For each network, all connections associated with parcels from a single functional network (e.g. within the CO and between the CO and the rest of the brain, Supplementary Fig. S1) were sub-selected and these features were then permuted in the test set as described above. To ensure that the impact of permuting the FC of a given network was due to network identity and not network size, the impact of permuting a matched set of randomly selected connections was also examined. For each network, we generated a matched set of functional connections randomly selected from the matrix and these features were then permuted in the test set. Fifty matched randomly selected feature sets were generated for each network. *P*-values were calculated for each network by comparing age prediction (R^2) when features from a single network were permuted and when randomly selected features were permuted. False discovery rate was used to correct for the multiple comparisons (12 networks).

Blocks of within-network and between-network connections

"Blocks" of FC comprised of either all connections among the parcels within a single network (e.g. within CO) or all connections between the parcels from 2 different networks (e.g. CO-to-VIS) were sub-selected and these features were then permuted in the test set as described above. To ensure that the impact of permuting the FC of a given block was due to the identity of the block and not the number of connections in a block, the impact of permuting a matched set of randomly selected connections was also examined. Fifty matched, randomly selected feature sets were generated for each block. *P*-values were calculated for each block by comparing age prediction (R^2) when features from a single block were permuted and when randomly selected features were permuted. False discovery rate was used to correct for the multiple comparisons (67 blocks).

Parcels

The connections associated with a single parcel (analogous to a seed map) were also selected and these features

Table 1. Variables potentially related to PMA in the eLABE and validation samples.

	eLABE sample N = 262; 53% males; 37% white		Validation sample N = 50; 58% males; 19% white	
PMA at scan (weeks)	41.8 (1.3); 38.6–45.4		41.8 (1.6); 38.4–45.9	
	Mean (std); min-max	*Correlation w/ PMA at scan*	*Mean (std); min-max*	*Correlation w/ PMA at scan*
GA at birth (weeks)	38.5 (1.00); 37–41	$r = 0.39$; $P < 0.001$	38.4 (1.01); 36–41	$r = 0.39$; $P = 0.004$
Total brain size (cm^3)	360 (38); 253–486	$r = 0.51$; $P < 0.001$	353 (41); 281–437	$r = 0.61$; $P < 0.001$
Cortical folding (gyrification index)	1.98 (0.091); 1.72–2.22	$r = 0.47$ $P < 0.001$	2.00 (0.083); 1.78–2.19	$r = 0.59$; $P < 0.001$
Amount of low motion data (minutes)	16.6 (4.4); 10.1–41.9	$r = -0.076$; $P = 0.22$	16.5 (4.5); 10.2–29.6	$r = 0.15$; $P = 0.29$
Head motion (frame displacement, mm)	0.078 (0.022); 0.036–0.15	$r = -0.13$; $P = 0.04$	0.087 (0.022); 0.044–0.14	$r = -0.30$; $P = 0.037$

were then permuted in the test set as described above. The impact of permuting a matched set of randomly selected connections was also examined. Five hundred matched randomly selected feature sets were generated as the null for all parcels. *P*-values were calculated for each parcel by comparing age prediction (R^2) when features from a single parcel are permuted and when randomly selected features are permuted. False Discovery Rate was used to correct for the multiple comparisons (333 parcels).

Results

Healthy, full-term infants ($n = 262$) were imaged during natural sleep without sedation within the first month of life (PMA: mean = 41.8; std = 1.25; range = 38–45 weeks) as a part of the Early Life Adversity, Biological Embedding, and Risk for Developmental Precursors of Mental Disorders (eLABE) cohort. More detailed health and demographic characteristics of the eLABE sample are reported in Supplementary Table S1. An additional set of healthy, full-term infants ($n = 50$) were imaged as a part of separate studies (CUDDEL + O2P2, see Methods and materials) using identical imaging parameters and procedures at similar ages (PMA: mean = 41.8; std = 1.66; range = 38–45 weeks) and were used to validate the generalizability of detectable patterns of FC related to PMA during the first month of life. Among these infants, PMA at scan was correlated with GA at birth, total brain size, cortical folding, and also weakly related to estimates of head motion and other demographic variables (Table 1).

Early development of brain systems can be detected over the first month of life

Linear SVR—a multivariate pattern classification technique (Smyser et al. 2016a; Nielsen et al. 2019)—was implemented to detect patterns of FC across the brain that varied with age over the first month of life within the eLABE sample. Multivariate patterns of brain-wide FC (i.e. all 55,278 functional connection among 333 parcels) identified with SVR were able to predict differences in PMA at scan of neonates ($R^2 = 0.51$, Fig. 2A) better than expected by chance ($P < 0.001$), even within the narrow window of development studied here (38–45 weeks; see Supplement 1 for results with additional parcellation schemes). Importantly, these patterns of brain-wide FC identified in the eLABE sample were generalizable and also predicted PMA at scan in the independent validation sample ($R^2 = 0.59$, Fig. 2B). Similar performance was observed when age prediction was repeated with 100 different partitions of the eLABE dataset into training and testing sets (Supplementary Fig. S3).

Further, age prediction from FC could not be entirely explained by age-related covariates or other factors with the potential to influence estimates of FC (e.g. connection length and head motion). GA at birth, total brain volume, cortical folding, and head motion could be predicted from FC (Supplement 2; Table S2), but prediction of these variables was poorer than age prediction from FC (Supplement 2; Table S2). More conservative frame censoring (FD < 0.15, FD < 0.10) further diminished the prediction of head motion from FC but did not impact age prediction (Supplement 3), suggesting that head motion did not explain the relation between brain maturity and FC. When these variables (head motion, amount of data, brain size, and cortical folding) were regressed out of the dataset, the residuals still significantly predicted PMA at scan in the eLABE sample ($R^2 = 0.31$; Fig. 2C) and in the validation sample ($R^2 = 0.34$; Fig. 2D). Similar performance was observed when this covariate regression procedure was repeated with 100 different partitions of the eLABE dataset into training and testing sets (Supplementary Fig. S3). This reduction in prediction was primarily a result of controlling for brain morphometry (intracranial volume and cortical folding) rather than as a result of controlling for data quality (head motion and amount of data; Supplement 2, Table S3). However, brain morphometry could not entirely explain the observed maturation in FC over the first month of life as age prediction based on

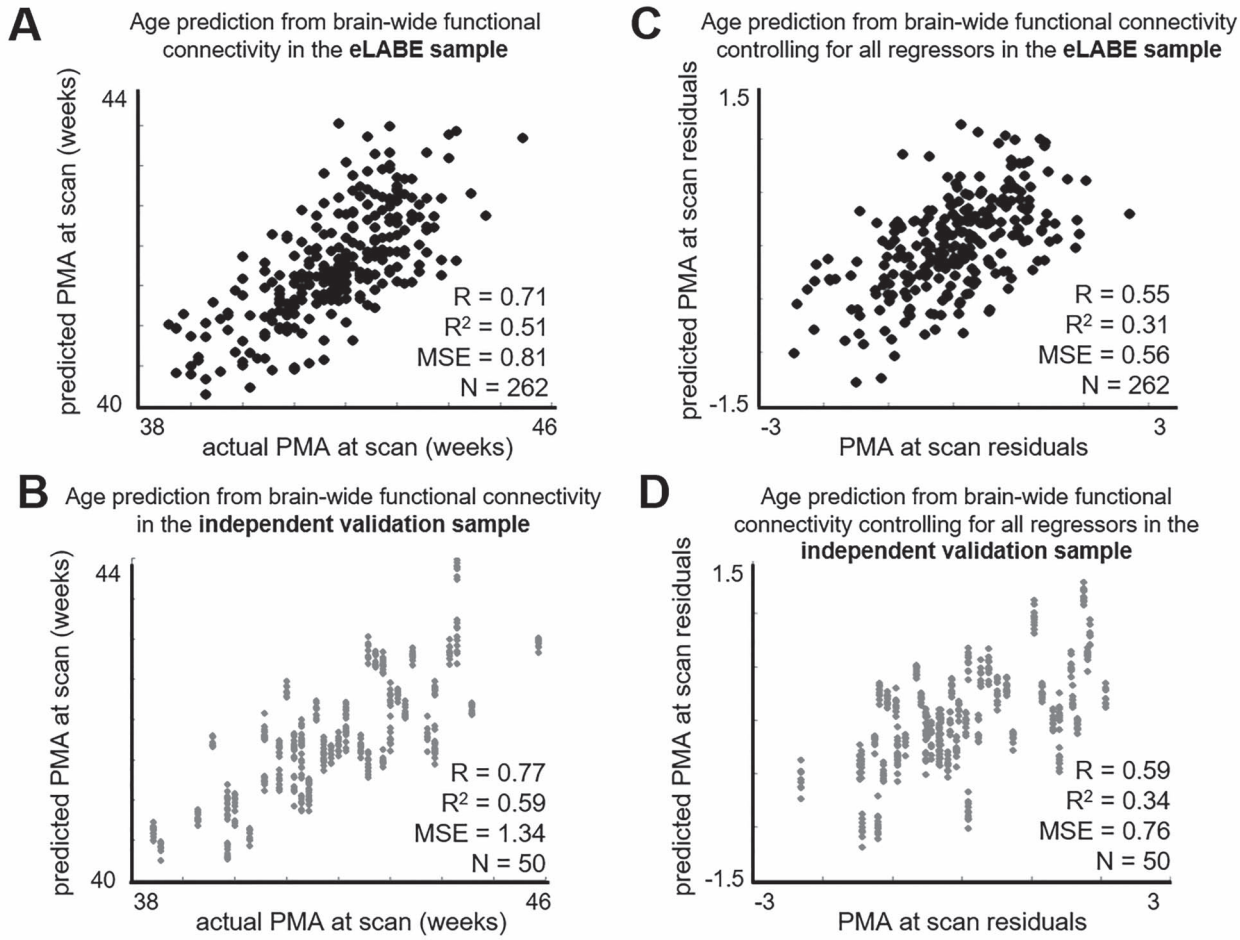

Fig. 2. A) Age prediction from brain-wide FC (333 parcels; 55,278 connections) in the eLABE sample obtained from a single train-test partition. Predicted ages based on FC were generated through 10-fold cross-validation. In turn, 10% of the sample was kept aside and the remaining 90% of the sample was used to identify patterns of FC related to PMA at scan, generating 10 separate models. The 10% of the sample that was left out of training was then used for testing such that each subject in the entire eLABE sample has a predicted PMA at scan. **B)** Age prediction from brain-wide FC in the validation sample using the models generated in the eLABE sample from a single train-test partition. Predicted ages based on FC for the validation sample were generated for each of the 10 models generated through SVR and 10-fold cross-validation in the eLABE sample. Thus, each subject in the validation sample has 10 predicted PMA at scan. **C)** Age prediction from brain-wide functional connecting when controlling for head motion (pre- and post-censoring mean FD), amount of data, head size (intracranial volume), and cortical folding (gyrification index) in the eLABE sample obtained from a single train-test partition. **D)** Age prediction from brain-wide FC in the validation sample using the models controlling for these regressors in the eLABE sample from a single train-test partition.

individual differences in FC outperformed age prediction based on individual differences in the distance between parcels (i.e. connection length; Supplement 4). Taken together, these findings provide evidence of reproducible developmental change across large-scale brain systems in the initial weeks of life.

Each individual functional network can predict age over the first month of life, but age prediction varies by functional network

Does the development of FC during the neonatal period differ across the brain and is it constrained by the large-scale organization of brain systems? Functional connectivity from each individual functional network could predict differences in PMA within the neonatal period better than expected by chance (range: $R^2 = 0.18$–0.47, $P < 0.001$), suggesting that both early and later developing brain systems undergo changes during this critical phase of development. Prediction of PMA differed between functional networks, but was highly correlated with network size ($r = 0.89$, $P < 0.001$; Fig. 3A). When FC measures were sub-selected from the same number of parcels from each functional network, prediction of PMA still differed between functional networks (Fig. 3B and Supplementary Fig. S4). After controlling for network size in this manner, early developing brain systems, on average, predicted age within the neonatal period better than late developing brain systems (Fig. 3C and Supplementary Fig. S5). The improved ability to discriminate slight differences in age when using FC from certain functional networks may be indicative of the relatively faster development occurring in these brain systems during the neonatal period. Importantly, FC from any single network did not outperform prediction of PMA from brain-wide FC ($R^2 = 0.51$) or from FC using a matched number of functional connections randomly selected

from multiple functional networks (Fig. 3D). As such, no single brain system, either early or late developing, was sufficient to optimally characterize the maturity of an individual neonate.

Age prediction worsens without FC from early developing sensorimotor networks or the cingulo-opercular network

These findings suggest that development of FC over the first month of life is occurring brain-wide, such that the developmental status of multiple functional networks contributes to the most accurate estimates of the maturity of an individual neonate. What would happen if a single brain system were removed? Disrupting the FC from early developing sensorimotor networks (visual, somatomotor—hand, somatomotor—mouth, auditory) and one later developing functional network (cingulo-opercular) negatively impacted age prediction from brain-wide FC more than expected by chance (Fig. 4B), suggesting that these networks contain unique developmental information for age prediction not represented elsewhere in the brain. In line with the finding that FC from multiple functional networks facilitate age prediction, the magnitude of the effect was small—the largest difference between the prediction of age from actual FC vs. permuted FC was only $R^2 = 0.06$. However, disrupting FC from these functional networks had a significant impact on age prediction when compared to disrupting FC that was randomly selected from multiple functional networks. Disrupting developmental information did not always significantly impact age prediction, indicating that information for age prediction from that network was redundant and present elsewhere in developing brain-wide FC (e.g. default-mode network, Fig. 4B). Developing FC from sensorimotor and cingulo-opercular functional networks differed from the development of FC occurring elsewhere in the brain, potentially resulting from unique combinations of different neurodevelopmental mechanisms.

This approach was extended to target and separately disrupt only within-network connections (i.e. connections among parcels within the same functional network) or between-network connections (i.e. connections between the parcels from 2 separate functional networks). Patterns of FC used for age prediction among early developing sensorimotor networks and the later developing cingulo-opercular network were again unique such that age prediction worsened without this developmental information (Fig. 4C and Supplementary Fig. S6). Disrupting within-network connections from the visual, auditory, somatomotor-hand, somatomotor-mouth, and cingulo-opercular networks significantly impeded age prediction from whole-brain FC. Only 1 block of between-network connections that did not involve either early developing sensorimotor networks or the cingulo-opercular network was uniquely important for age prediction (parietal memory to dorsal attention; Fig. 4C). FC from all of the blocks that were uniquely important for age prediction were examined and several consistent developmental patterns were noted including (i) increased connectivity strength of within-network connections with PMA at scan in all but the somatosensory networks, (ii) more strongly negative connectivity with PMA in the blocks of connections between the default-mode and sensorimotor networks, and (iii) more mixed increases/decreases in connectivity strength with PMA in between-network connections (Supplementary Fig. S7).

To address potential bias from the definitions of functional networks derived in adults (Bryce et al. 2021), this approach was modified to disrupt only connections associated with a single parcel (i.e. analogous to a seed map), independent of a priori network definitions. This approach was also applied to 2 additional parcellation schemes to control for any potential bias at the parcel level (Supplement 1). In these analyses, disrupting FC from regions belonging to early developing brain systems (primary visual, auditory, somatosensory, and motor cortices) and the cingulo-opercular network (anterior insula and mid-cingulate) impeded the prediction of PMA (Fig. 4D) and these findings were independent of parcellation (Supplementary Fig. S8).

Discussion

The goal of this study was to track the development of large-scale brain systems over the first month of life. Our findings indicate that there are rapid and widespread changes in large-scale brain systems during the neonatal period and that FC can detect evidence of developmental change within this narrow developmental window. Brain-wide patterns of FC were able to predict PMA at scan well and, importantly, generalized to an independently collected validation sample. Each individual functional network also predicted PMA, suggesting that developing FC was present across all functional networks during the neonatal period. However, the FC involving sensorimotor networks and the cingulo-opercular network facilitated better prediction of differences in PMA within the neonatal period and contained unique developmental information for age prediction. Our findings shed new light on the relative rate and scope of the development of brain systems during the neonatal period as well as bolster the promise of fc-MRI to facilitate the early detection and/or prevention of atypical neurodevelopment.

Neonatal development occurs brain-wide in both early and late developing brain systems

Our findings suggest that the neurodevelopmental processes taking place after birth occur brain-wide such that the development change in FC over the first month of life is detectable in each large-scale brain system. After birth, the brain matures by several different mechanisms (e.g. increasing myelination, axonal pruning, synaptogenesis, synaptic pruning, changes in ion channel function, and changes in gene expression; Sydnor et al. 2021), and the postnatal environment and experience can begin

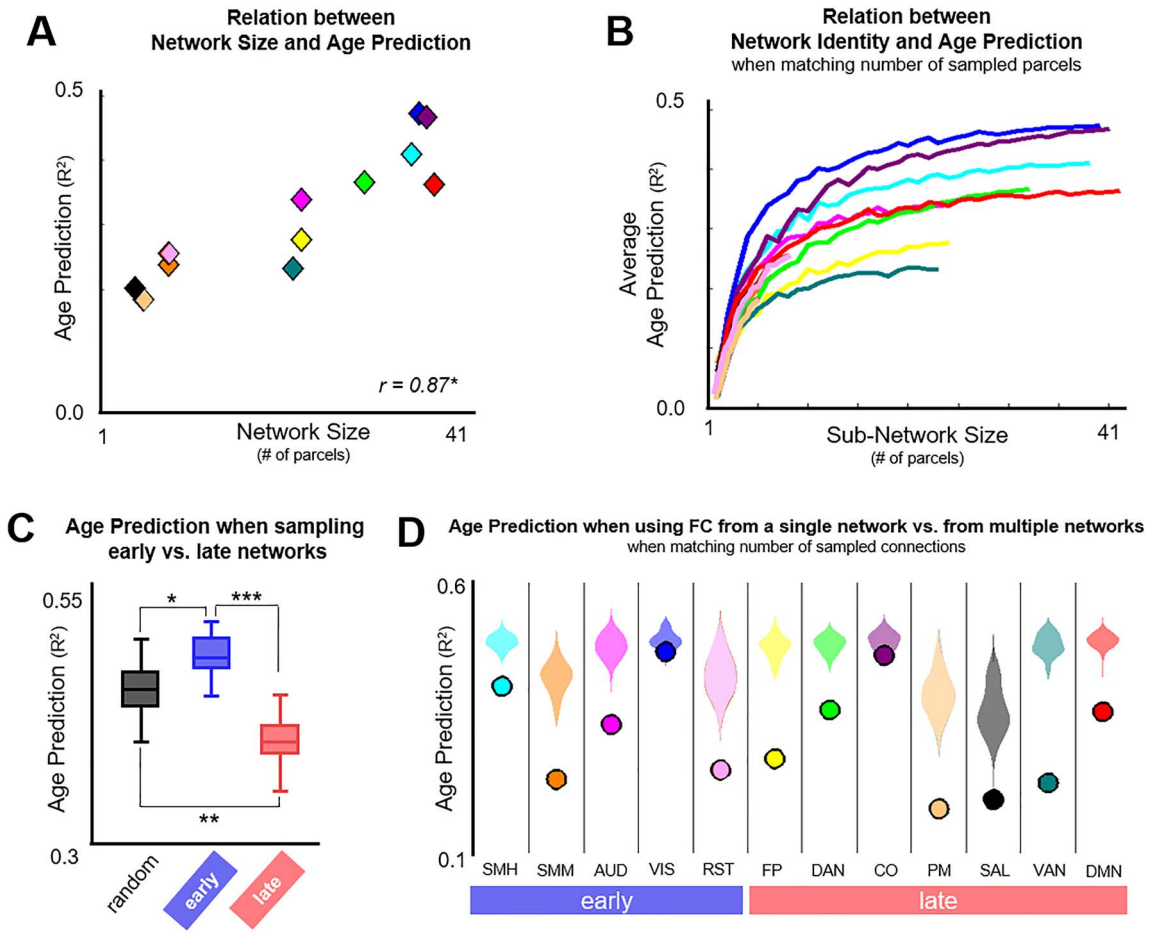

Fig. 3. A) The relation between age prediction and network size when using only FC involving a single functional network to predict age. Patterns of FC related to PMA at scan involving parcels from a single functional network were identified with SVR in the eLABE sample. Variance explained (R^2) was quantified by comparing the predicted ages based on FC from a single network and true ages of the eLABE sample. **B)** The relation between age prediction and network identity as a function of the number of parcels sampled from a single functional network. Patterns of FC related to PMA at scan involving a set number (e.g. 20) of randomly selected parcels from a single network were identified with SVR in the eLABE sample. This process was repeated 50 times for each possible subnetwork size for each functional network (e.g. 1–41 for the default-mode network, 1–4 for the salience network). Curves represent the average age prediction across the 50 random repetitions. The full distribution of these curves is depicted in Supplementary Fig. S4. **C)** Comparison of the variance explained (R^2) when using FC sampled from early vs. late developing functional networks for age prediction. The results when 50 parcels were sampled are depicted here and the results when fewer parcels were sampled are depicted in Supplementary Fig. S5. Statistical comparison of age prediction was determine by Steiger's *t*-test for comparing elements of a correlation matrix. A Steiger's *t*-statistic that is larger than 1.95 indicates a *P*-value < 0.05. Asterisks indicate that the difference in age prediction observed between the 2 types of feature sets (random, early, or late) generated a Steiger's *t*-statistic that was >1.95 for 28% (*), 46% (**), and 78% (***) of the tested pairs. **D)** Comparison of the variance explained (R^2) when using only FC from a single network to predict age (circle) and the variance explained when using FC from a matched number (per each individual functional network) of randomly selected connections from multiple networks to predict age (violin distribution). For each functional network, 50 randomly selected feature sets were generated and patterns of FC related to PMA at scan were identified with SVR. Variance explained (R^2) was quantified by comparing the predicted ages based on FC from either a single network or randomly selected connections and true ages of the eLABE sample. Functional networks were grouped according to early (light blue) and late (light red) developing brain systems.

to directly influence brain development (Dawson et al. 2000). Developing FC during the neonatal period was present in both early and late developing brain systems, demonstrating the scope of the potential impact of early development on functional brain organization. Even though the FC from sensorimotor networks appears the most mature in infancy (Fransson et al. 2007; Lin et al. 2008; Gao et al. 2009, 2015; Doria et al. 2010; Smyser et al. 2010; Eyre et al. 2021), development is ongoing during the neonatal period across all functional networks. Furthermore, the presence of developing FC during the neonatal period in late developing brain systems suggests that maturation, environment, and experience during this critical developmental window may also shape the function and subsequent development of late developing brain systems in which behavioral capacities are not yet observable.

Developing FC differed in early developing brain systems, potentially due to rapid maturation and unique neurobiological mechanisms

Developing FC differed in early developing sensorimotor networks (and the cingulo-opercular network) such that the developmental change in these functional networks was more pronounced and they were differentially important for age prediction. Many developmental

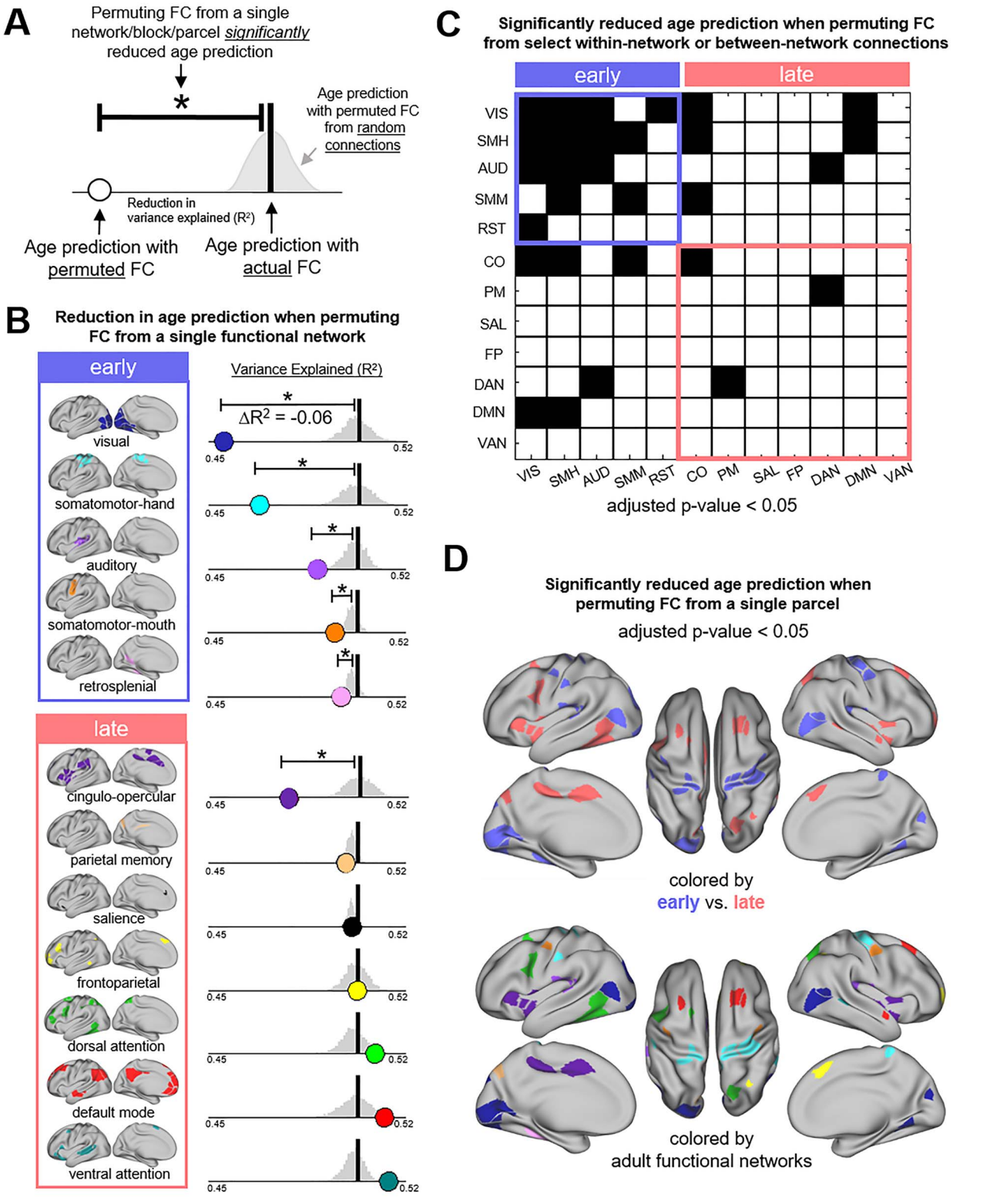

Fig. 4. A) Schematic of the comparison used to assess the unique importance of FC from a single network, block, or parcel for prediction of age within the neonatal period. Connections from a single network, block, or parcel were randomly permuted before testing in each fold of cross-validation, removing any potential developmentally relevant information for prediction of PMA. Age prediction with this permuted FC (white circle) was then compared to age prediction with permuted FC from a matched set of randomly selected connections (gray distribution). Age prediction with actual FC (as depicted in Fig. 2A) is also provided for reference (black line). Functional networks, blocks, or parcels were considered uniquely important if disrupting their FC significantly impeded age prediction when compared to matched randomly selected connections and after correcting for multiple comparisons. **B)** Reduction in age prediction when permuting FC from a single functional network. **C)** Blocks of within-network and between-network FC that are uniquely important for age prediction. **D)** Parcels whose FC is uniquely important for age prediction colored by early vs. late developing and by functional networks as depicted in Fig. 1.

processes occur earlier and at a faster rate in sensorimotor brain systems, potentially enabling better prediction of an infant's age in comparison to other brain systems. During prenatal and postnatal development, synaptogenesis (Huttenlocher and Dabholkar 1997), dendritic growth and arborization (Travis et al. 2005), the myelination, growth, and functional refinement of thalamocortical connections (Flechsig Of Leipsic 1901; Toulmin et al. 2015), the myelination of intra-cortical connections (Miller et al. 2012), cortical expansion (Hill et al. 2010), and the refinement of cortical microstructure (Smyser et al. 2016c; Natu et al. 2021) occur earlier and more rapidly in sensorimotor cortices than in association cortices. The rapid maturation of brain systems important for sensorimotor function coincides with the sensitive periods for visual, motor, and language development in which a child's experience can shape ongoing brain development (Johnson 2005; Lewis and Maurer 2005; Werker and Tees 2005). Since FC is thought to reflect a statistical history of co-activation across the lifespan (Lewis et al. 2009; Harmelech and Malach 2013; Shannon et al. 2016), it is possible that developing FC in sensorimotor brain systems can detect the rapid changes in the expression of sensorimotor behaviors that occur shortly after birth. The emergence of white matter tracts prenatally foreshadows subsequent maturation of functional networks as projection tracts involving sensorimotor brain systems (e.g. internal capsule, corona radiata, corticospinal tract, and thalamic radiations) are identifiable earlier than association tracts (e.g. interior longitudinal fasiculus, superior longitudinal fasiculus, and uncinate) (Ouyang et al. 2019). The rapid growth and refinement of thalamo-cortical fibers during the third trimester such that primary sensorimotor cortex (i.e. early developing brain systems) appears more refined that that of multimodal cortex (i.e. late developing brain systems; Huttenlocher and Dabholkar 1997; Travis et al. 2005; Petanjek et al. 2011) may potentially set the stage for differential rates of maturing brain function over the first month of life (Toulmin et al. 2015). The combination of differential changes to brain structure (Flechsig Of Leipsic 1901; Huttenlocher and Dabholkar 1997; Travis et al. 2005; Hill et al. 2010; Miller et al. 2012; Toulmin et al. 2015; Smyser et al. 2016c; Natu et al. 2021), gene expression (Kwan et al. 2012; Pletikos et al. 2014), and experience (Johnson; Lewis and Maurer 2005; Werker and Tees 2005) during gestation and infancy is unique to each sensorimotor brain system and potentially underlies the unique patterns of FC that were necessary for optimal prediction of PMA within the neonatal period. Our findings corroborate that there is differential development of early developing sensorimotor brain systems and these differences in maturation can be distinguished shortly after birth. Further work is needed to isolate the specific neurobiological processes contributing to the unique and rapid maturation of FC in sensorimotor networks during the neonatal period.

Developing FC from the cingulo-opercular network resembled early developing brain systems, highlighting a key role in early brain development

Even though the cingulo-opercular network exhibits extensive development later in childhood and adolescence (i.e. late developing) as children begin to acquire more sophisticated cognitive control strategies (Luna et al. 2015), rapid and unique development of the cingulo-opercular network was found over the first month of life, similar to early developing sensorimotor brain systems. When fully mature, the cingulo-opercular network (originally labeled the salience network by Seeley et al. 2007; see Uddin et al. 2019 for discussion of taxonomy) plays a crucial role in executive functioning and is important for detecting, responding to, and learning from errors (Neta et al. 2014; Roe et al. 2021), for pain/disgust processing (Nevian 2017; Sharvit et al. 2019), and for conflict monitoring (Carter et al. 1998; Botvinick et al. 1999). In particular, the insula plays a key role in the cingulo-opercular network integrating sensorimotor, chemical sensory, cognitive, and social–emotional processing (Kurth et al. 2010). It is possible that during this developmental period, the cingulo-opercular network is critical to learning the patterns of sensorimotor activity that code for errors, pain, and conflict later in development. Our results indicate that FC between the cingulo-opercular network and sensorimotor networks was important for capturing differences in maturity during the neonatal period (Fig. 4C). These results are consistent with structural studies of fetal brain development, which demonstrate the insula (part of the cingulo-opercular network) is first to undergo differentiation (Streeter et al. 1912), folding, and vascularization (Afif et al. 2007). Maturation of cortical microstructure emanates outward from the insula during early gestation in nonhuman primates (Sidman 1982; Kroenke et al. 2007). Lastly, the anatomy and cytoarchitecture of regions in the cingulo-opercular network vary substantially across individuals in adulthood (Vogt et al. 1995); the current results indicate that FC of these regions matures in a unique and rapid manner over the first month of life suggesting that the individualization of functional networks might begin in infancy. Further work is needed to better elucidate the special role of the cingulo-opercular network in early brain development.

Functional connectivity MRI is a promising tool for evaluating neonatal brain maturity

This work has demonstrated that FC can be used to detect slight differences in age during the first month of life and may be a powerful neuroimaging tool to assay early brain maturity. This result, combined with studies of prematurely born infants identifying FC related to small differences in age (i.e. GA at birth from 28 to 40 weeks; Doria et al. 2010; Smyser et al. 2010, 2016a;

Ball et al. 2016), corroborate that FC is a sensitive indicator of brain development during infancy. In the eLABE sample, estimates of age from resting-state functional MRI were more accurate and sensitive ($R^2 = 0.51$) than estimates from total brain volume ($R^2 = 0.25$) or cortical folding ($R^2 = 0.23$), demonstrating the added value of assessing brain function. When PMA was split into prenatal and postnatal components (i.e. gestational age at birth and weeks between birth and scan), FC could better predict postnatal maturation (weeks between birth and scan: $R^2 = 0.35$) than prenatal maturation (GA at birth: $R^2 = 0.10$; Supplement 2), providing further evidence that FC continues to mature after birth and may be influenced by postnatal experience and environment. The potential clinical utility of estimates of brain maturity using FC is also bolstered by our demonstration of the generalizability of age prediction in an independently collected validation sample composed of newborns that were studied independently, but in a similar manner (e.g. procedures, sequences, scanner, and site). This demonstration of a robust, normative brain "growth curve" during infancy is a crucial first step towards clinical translation, the identification of atypical brain maturity, and investigation of the impact of protective or deleterious experiences on early brain development. Deviations from expected brain maturity estimated from neuroimaging have been used to indicate clinical impairment in adolescence (Nielsen et al. 2020a; Parkes et al. 2021), but future work remains necessary to determine the clinical significance and predictive value of deviations from expected brain maturity in infancy.

Limitations

Our findings should be viewed in light of the current study's limitations. First, the current study leveraged cross-sectional differences in PMA across neonates to track the development of large-scale brain systems over the first month of life, but it did not directly examine longitudinal developmental changes in brain systems. As such, individual developmental trajectories of brain systems may differ from the cross-sectional developmental differences described in this work. Second, our ability to assay brain maturity is limited by the precision of estimates of an infant's maturity. The date of an infant's conception is difficult to determine (except in the case of in vitro fertilization) such that GA at birth is an estimate within ± 2 weeks of the true maturity of the newborn. Furthermore, multivariate pattern classification techniques are a powerful tool to detect subtle and complex differences in neuroimaging data, but also come with a set of challenges (Cui and Gong 2018; Bzdok and Ioannidis 2019; Davatzikos 2019; Nielsen et al. 2020b). Because these approaches are sensitive to multivariate patterns but are agnostic to the source of these patterns, the observed age prediction from FC could be artificially enhanced by variation in FC attributable to age-related confounding variables (Nielsen et al. 2020b). This study demonstrated that prediction of PMA within the neonatal period using FC was not driven entirely by confounding variables like brain size, cortical folding, or head motion (Supplement 2), but it is possible that other unknown or unmeasured variables are contributing to our observed age prediction. Because the infant FC was acquired during sleep, it is possible that age-related changes in sleep activity or sleep stage may produce differences in FC and might facilitate age prediction. Although this study employed cutting-edge surface-based strategies to process the infant resting-state fMRI, aligning these data with an adult template may not be ideal (Gaillard et al. 2001; Kazemi et al. 2007) and may have consequences for age prediction because of the neuroanatomical differences between infants and adults. These findings should be replicated as infant atlases become more available (Dufford et al. 2022). In addition, though several approaches were employed to demonstrate the importance of different functional networks for age prediction, the multivariate nature of pattern classification techniques makes it difficult to truly isolate and interpret what specific functional connections enable age prediction (Nielsen et al. 2020b). Lastly, brain systems and parcels were defined according to the functional network organization of healthy adults (Power et al. 2011; Gordon et al. 2016). Even though consistent results were identified when examining developing FC at the parcel level (Fig. 4D) and across 2 additional parcellations (Supplement 1), it is possible that the development of FC during infancy may better align with functional networks and/or parcellation schemes defined in infants Bryce et al. 2021.

In summary, the current study reveals that the development of large-scale brain systems over the first month of life involves the complex coordination of multiple brain systems. During this foundational developmental window marked by rapid maturation, novel experiences, and heightened plasticity, developing FC was present brain-wide, highlighting the potential cascading impact of atypical brain maturation during infancy. Early brain development appeared to be constrained by the large-scale brain organization and the different functions and behaviors these neural systems support. These observations highlight the promise of fc-MRI as a tool for investigators wanting to study the neural mechanisms underlying the early development of large-scale brain systems and for clinicians desiring to detect atypical brain development early to prevent negative outcomes.

Acknowledgments

The authors thank Karen Lukas and Rich Nagel for assistance with scanning neonates and Arpana Agrawal for sharing data from the CUDDEL study.

Supplementary material

Supplementary material is available at *Cerebral Cortex* online.

Funding

This research was supported by National Institute of Health (grant nos. R01 MH121877 to L.S.W., J.L.L., C.E.R., R01 DA046224 to C.E.R. and C.D.S, K23 MH109983 to C.M.S., R01 MH122389 to C.M.S., K02 NS089852 to C.D.S., R01 MH113570 to C.D.S. and C.E.R., and R01 MH113883 to C.D.S., J.L.L. and B.W.W.); Intellectual and Developmental Disabilities Research Center (P50 HD103525 to C.D.S., C.E.R., and J.S.S.; K23 MH105179 to C.E.R.; R01 MH090786 to D.M.B.); the McDonnell Center for Systems Neuroscience (C.M.S.); the Taylor Family Institute (C.M.S.); the Parker Fund (C.M.S.); the Foundation for Society of Maternal-Fetal Medicine (N.R.); the American Association of Obstetricians and Gynecologists Foundation Scholars Award (N.R.); the March of Dimes Foundation; and institutional support from St. Louis Children's Hospital, Barnes-Jewish Hospital, and Washington University in St. Louis School of Medicine.

Conflict of interest statement: None declared.

References

Afif A, Bouvier R, Buenerd A, Trouillas J, Mertens P. Development of the human fetal insular cortex: study of the gyration from 13 to 28 gestational weeks. *Brain Struct Funct*. 2007:212(3–4):335–346.

Avishai-Eliner S, Brunson KL, Sandman CA, Baram TZ. Stressed-out, or in (utero)? *Trends Neurosci*. 2002:25(10):518–524.

Ball G, Aljabar P, Arichi T, Tusor N, Cox D, Merchant N, Nongena P, Hajnal JV, Edwards AD, Counsell SJ. Machine-learning to characterise neonatal functional connectivity in the preterm brain. *NeuroImage*. 2016:124(Pt A):267–275.

Bateman BT, Mhyre JM, Hernandez-Diaz S, Huybrechts KF, Fischer MA, Creanga AA, Callaghan WM, Gagne JJ. Development of a comorbidity index for use in obstetric patients. *Obstet Gynecol*. 2013:122(5):957–965.

Bick J, Nelson CA. Early adverse experiences and the developing brain. *Neuropsychopharmacology*. 2015:41(1):177–196.

Biswal B, Yetkin FZ, Haughton VM, Hyde JS. Functional connectivity in the motor cortex of resting human brain using echo-planar MRI. *Magn Reson Med*. 1995, 1995:34(4):537–541.

Botvinick M, Nystrom LE, Fissell K, Carter CS, Cohen JD. Conflict monitoring versus selection-for-action in anterior cingulate cortex. *Nature*. 1999:402(6758):179–181.

Bryce NV, Flournoy JC, Guassi Moreira JF, Rosen ML, Sambook KA, Mair P, McLaughlin KA. Brain parcellation selection: an overlooked decision point with meaningful effects on individual differences in resting-state functional connectivity. *NeuroImage*. 2021:243:118487.

Bzdok D, Ioannidis JPA. Exploration, inference, and prediction in neuroscience and biomedicine. *Trends Neurosci*. 2019:42(4):251–262.

Carter CS, Braver TS, Barch DM, Botvinick MM, Noll D, Cohen JD. Anterior cingulate cortex, error detection, and the online monitoring of performance. *Science*. 1998:280(5364):747–749.

Chen Y, Baram TZ. Toward understanding how early-life stress reprograms cognitive and emotional brain networks. *Neuropsychopharmacology*. 2015:41(1):197–206.

Cui Z, Gong G. The effect of machine learning regression algorithms and sample size on individualized behavioral prediction with functional connectivity features. *NeuroImage*. 2018:178:622–637.

Davatzikos C. Machine learning in neuroimaging: progress and challenges. *NeuroImage*. 2019:197:652–656.

Dawson G, Ashman SB, Carver LJ. The role of early experience in shaping behavioral and brain development and its implications for social policy. *Dev Psychopathol*. 2000:12(4):695–712.

Doria V, Beckmann CF, Arichi T, Merchant N, Groppo M, Turkheimer FE, Counsell SJ, Murgasova M, Aljabar P, Nunes RG, et al. Emergence of resting state networks in the preterm human brain. *Proc Natl Acad Sci*. 2010:107(46):20015–20020.

Dosenbach NUF, Nardos B, Cohen AL, Fair DA, Power JD, Church JA, Nelson SM, Wig GS, Vogel AC, Lessov-Schlaggar CN, et al. Prediction of individual brain maturity using fMRI. *Science*. 2010:329(5997):1358–1361.

Duerden EG, Card D, Lax ID, Donner EJ, Taylor MJ. Alterations in frontostriatal pathways in children born very preterm. *Dev Med Child Neurol*. 2013:55(10):952–958.

Dufford, Alexander, et al. (Un)common space in infant neuroimaging studies: A systematic review of infant templates. *Human Brain Mapping*. 2022:43(9):3007–3016.

Eyre M, Fitzgibbon SP, Ciarrusta J, Cordero-Grande L, Price AN, Poppe T, Schuh A, Hughes E, O'Keeffe C, Brandon J, et al. The Developing Human Connectome Project: typical and disrupted perinatal functional connectivity. *Brain*. 2021:144(7):2199–2213.

Flechsig Of Leipsic P. Developmental (myelogenetic) localisation of the cerebral cortex in the human subject. *Lancet*. 1901:158(4077):1027–1030.

Fransson P, Skiöld B, Horsch S, Nordell A, Blennow M, Lagercrantz H, Åden U. Resting-state networks in the infant brain. *Proc Natl Acad Sci*. 2007:104(39):15531–15536.

Gaillard, William Davis, Cecile B. Grandin, and Benjamin Xu. Developmental aspects of pediatric fMRI: considerations for image acquisition, analysis, and interpretation. *Neuroimage*. 2001:13(2):239–249.

Gao W, Zhu H, Giovanello KS, Smith JK, Shen D, Gilmore JH, Lin W. Evidence on the emergence of the brain's default network from 2-week-old to 2-year-old healthy pediatric subjects. *Proc Natl Acad Sci*. 2009:106(16):6790–6795.

Gao W, Alcauter S, Elton A, Hernandez-Castillo CR, Smith JK, Ramirez J, Lin W. Functional network development during the first year: relative sequence and socioeconomic correlations. *Cereb Cortex*. 2015:25(9):2919–2928.

Gordon EM, Laumann TO, Adeyemo B, Huckins JF, Kelley WM, Petersen SE. Generation and evaluation of a cortical area parcellation from resting-state correlations. *Cereb Cortex*. 2016:26(1):288–303.

Gratton C, Nomura EM, Pérez F, D'Esposito M. Focal brain lesions to critical locations cause widespread disruption of the modular organization of the brain. *J Cogn Neurosci*. 2012:24(6):1275–1285.

Harmelech T, Malach R. Neurocognitive biases and the patterns of spontaneous correlations in the human cortex. *Trends Cogn Sci*. 2013:17(12):606–615.

Hill J, Inder T, Neil J, Dierker D, Harwell J, van Essen D. Similar patterns of cortical expansion during human development and evolution. *Proc Natl Acad Sci*. 2010:107(29):13135–13140.

Huttenlocher PR, Dabholkar AS. Regional differences in synaptogenesis in human cerebral cortex. *J Comp Neurol*. 1997:387(2):167–178.

Johnson MH. Sensitive periods in functional brain development: problems and prospects. *Dev Psychobiol*. 2005:46(3):287–292.

Kazemi, Kamran, et al. A neonatal atlas template for spatial normalization of whole-brain magnetic resonance images of newborns: preliminary results. *Neuroimage*. 2007:37(2):463–473.

Knudsen EI. Sensitive periods in the development of the brain and behavior. *J Cogn Neurosci*. 2004:16(8):1412–1425.

Kroenke CD, van Essen DC, Inder TE, Rees S, Bretthorst GL, Neil JJ. Microstructural changes of the baboon cerebral cortex during gestational development reflected in magnetic resonance imaging diffusion anisotropy. *J Neurosci*. 2007:27(46):12506–12515.

Kurth F, Zilles K, Fox PT, Laird AR, Eickhoff SB. A link between the systems: functional differentiation and integration within the human insula revealed by meta-analysis. *Brain Struct Funct*. 2010:214(5–6):519–534.

Kwan KY, Šestan N, Anton ES. Transcriptional co-regulation of neuronal migration and laminar identity in the neocortex. *Development*. 2012:139(9):1535–1546.

LaMantia AS, Rakic P. Axon overproduction and elimination in the corpus callosum of the developing rhesus monkey. *J Neurosci*. 1990:10(7):2156–2175.

Lebel C, Treit S, Beaulieu C. A review of diffusion MRI of typical white matter development from early childhood to young adulthood. *NMR Biomed*. 2019:32(4):e3778.

Lewis TL, Maurer D. Multiple sensitive periods in human visual development: evidence from visually deprived children. *Dev Psychobiol*. 2005:46(3):163–183.

Lewis CM, Baldassarre A, Committeri G, Romani GL, Corbetta M. Learning sculpts the spontaneous activity of the resting human brain. *Proc Natl Acad Sci U S A*. 2009:106(41):17558–17563.

Lin W, Zhu Q, Gao W, Chen Y, Toh C-H, Styner M, Gerig G, Smith JK, Biswal B, Gilmore JH. Functional connectivity MR imaging reveals cortical functional connectivity in the developing brain. *Am J Neuroradiol*. 2008:29(10):1883–1889.

Luna B, Marek S, Larsen B, Tervo-Clemmens B, Chahal R. An integrative model of the maturation of cognitive control. *Annu Rev Neurosci*. 2015:38(1):151–170.

Marek S, Hwang K, Foran W, Hallquist MN, Luna B. The contribution of network organization and integration to the development of cognitive control. *PLoS Biol*. 2015:13(12):e1002328.

Marek S, Tervo-Clemmens B, Nielsen AN, Wheelock MD, Miller RL, Laumann TO, Earl E, Foran WW, Cordova M, Doyle O, et al. Identifying reproducible individual differences in childhood functional brain networks: an ABCD study. *Dev Cogn Neurosci*. 2019:40:100706.

Miller DJ, Duka T, Stimpson CD, Schapiro SJ, Baze WB, McArthur MJ, Fobbs AJ, Sousa AMM, Šestan N, Wildman DE, et al. Prolonged myelination in human neocortical evolution. *Proc Natl Acad Sci*. 2012:109(41):16480–16485.

Monk C, Lugo-Candelas C, Trumpff C. Prenatal developmental origins of future psychopathology: mechanisms and pathways. *Annu Rev Clin Psychol*. 2019:15(1):317–344.

Natu VS, Rosenke M, Wu H, Querdasi FR, Kular H, Lopez-Alvarez N, Grotheer M, Berman S, Mezer AA, Grill-Spector K. Infants' cortex undergoes microstructural growth coupled with myelination during development. *Commun Biol*. 2021:4(1):1191.

Neta M, Schlaggar BL, Petersen SE. Separable responses to error, ambiguity, and reaction time in cingulo-opercular task control regions. *NeuroImage*. 2014:99:59–68.

Nevian T. The cingulate cortex: divided in pain. *Nat Neurosci*. 2017:20(11):1515–1517.

Newbold DJ, Laumann TO, Hoyt CR, Hampton JM, Montez DF, Raut RV, Ortega M, Mitra A, Nielsen AN, Miller DB, et al. Plasticity and spontaneous activity pulses in disused human brain circuits. *Neuron*. 2020:107(3):580–589.e6.

Newbold DJ, Gordon EM, Laumann TO, Seider NA, Montez DF, Gross SJ, Zheng A, Nielsen AN, Hoyt CR, Hampton JM, et al. Cingulo-opercular control network and disused motor circuits joined in standby mode. *Proc Natl Acad Sci*. 2021:118(13). https://doi.org/10.1073/pnas.2019128118.

Nielsen AN, Greene DJ, Gratton C, Dosenbach NUF, Petersen SE, Schlaggar BL. Evaluating the prediction of brain maturity from functional connectivity after motion artifact denoising. *Cereb Cortex*. 2019:29(6):2455–2469.

Nielsen AN, Gratton C, Church JA, Dosenbach NUF, Black KJ, Petersen SE, Schlaggar BL, Greene DJ. Atypical functional connectivity in tourette syndrome differs between children and adults. *Biol Psychiatry*. 2020a:87(2):164–173.

Nielsen AN, Barch DM, Petersen SE, Schlaggar BL, Greene DJ. Machine learning with neuroimaging: evaluating its applications in psychiatry. *Biol Psychiatry*. 2020b:5(8):791–798.

Ouyang M, Dubois J, Yu Q, Mukherjee P, Huang H. Delineation of early brain development from fetuses to infants with diffusion MRI and beyond. *NeuroImage*. 2019:185:836–850.

Parkes L, Moore TM, Calkins ME, Cook PA, Cieslak M, Roalf DR, Wolf DH, Gur RC, Gur RE, Satterthwaite TD, et al. Transdiagnostic dimensions of psychopathology explain individuals' unique deviations from normative neurodevelopment in brain structure. *Transl Psychiatry*. 2021:11(1):1–13.

Petanjek Z, Judaš M, Šimić G, Rašin MR, Uylings HB, Rakic P, Kostović I. Extraordinary neoteny of synaptic spines in the human prefrontal cortex. *Proc Natl Acad Sci*. 2011:108(32):13281–13286.

Pineda RG, Neil J, Dierker D, Smyser CD, Wallendorf M, Kidokoro H, et al. Alterations in brain structure and neurodevelopmental outcome in preterm infants hospitalized in different neonatal intensive care unit environments. *J Pediatr*. 2014:164(1):52–60.

Pletikos M, Sousa AMM, Sedmak G, Meyer KA, Zhu Y, Cheng F, Li M, Kawasawa YI, Šestan N. Temporal specification and bilaterality of human neocortical topographic gene expression. *Neuron*. 2014:81(2):321–332.

Power JD, Cohen AL, Nelson SM, Wig GS, Barnes KA, Church JA, Vogel AC, Laumann TO, Miezin FM, Schlaggar BL, et al. Functional network organization of the human brain. *Neuron*. 2011:72(4):665–678.

Power JD, Barnes KA, Snyder AZ, Schlaggar BL, Petersen SE. Spurious but systematic correlations in functional connectivity MRI networks arise from subject motion. *NeuroImage*. 2012:59(3):2142–2154.

Power JD, Mitra A, Laumann TO, Snyder AZ, Schlaggar BL, Petersen SE. Methods to detect, characterize, and remove motion artifact in resting state fMRI. *NeuroImage*. 2014:84:320–341.

Roe MA, Engelhardt LE, Nugiel T, Harden KP, Tucker-Drob EM, Church JA. Error-signaling in the developing brain. *NeuroImage*. 2021:227:117621.

Satterthwaite TD, Wolf DH, Ruparel K, Erus G, Elliott MA, Eickhoff SB, Gennatas ED, Jackson C, Prabhakaran K, Smith A, et al. Heterogeneous impact of motion on fundamental patterns of developmental changes in functional connectivity during youth. *NeuroImage*. 2013:83:45–57.

Schaefer A, Kong R, Gordon EM, Laumann TO, Zuo X-N, Holmes AJ, Eickhoff SB, Yeo BTT. Local-global parcellation of the human cerebral cortex from intrinsic functional connectivity MRI. *Cereb Cortex*. 2018:28(9):3095–3114.

Seeley, William W., et al. Dissociable intrinsic connectivity networks for salience processing and executive control. *Journal of Neuroscience*. 2007:27(9):2349–2356.

Shannon BJ, Vaishnavi SN, Vlassenko AG, Shimony JS, Rutlin J, Raichle ME. Brain aerobic glycolysis and motor adaptation learning. *Proc Natl Acad Sci U S A*. 2016:113(26):E3782–E3791.

Sharvit G, Vuilleumier P, Corradi-Dell'Acqua C. Sensory-specific predictive models in the human anterior insula. *F1000Research*. 2019:8:164.

Shimony JS, Smyser CD, Wideman G, Alexopoulos D, Hill J, Harwell J, Dierker D, van Essen DC, Inder TE, Neil JJ. Comparison of cortical folding measures for evaluation of developing human brain. *NeuroImage*. 2016:125:780–790.

Sidman R. Development of the human central nervous system. In: *Histology and histopathology of the nervous system*; 1982

Smyser CD, Inder TE, Shimony JS, Hill JE, Degnan AJ, Snyder AZ, Neil JJ. Longitudinal analysis of neural network development in preterm infants. *Cereb Cortex*. 2010:20(12): 2852–2862.

Smyser CD, Inder TE, Shimony JS, Hill JE, Degnan AJ, Snyder AZ, Neil JJ. Functional connectivity MRI in infants: exploration of the functional organization of the developing brain. *Neuroimage*. 2011:56(3):1437–1452.

Smyser, Christopher D., et al. Resting-state network complexity and magnitude are reduced in prematurely born infants. *Cerebral cortex*. 2016:26(1):322–333.

Smyser CD, Dosenbach NUF, Smyser TA, Snyder AZ, Rogers CE, Inder TE, Schlaggar BL, Neil JJ. Prediction of brain maturity in infants using machine-learning algorithms. *NeuroImage*. 2016a: 136:1–9.

Smyser TA, Smyser CD, Rogers CE, Gillespie SK, Inder TE, Neil JJ. Cortical gray and adjacent white matter demonstrate synchronous maturation in very preterm infants. *Cereb Cortex*. 2016b:26(8): 3370–3378.

Steiger JH. Tests for comparing elements of a correlation matrix. *Psychol Bull*. 1980:87(2):245–251.

Stout MJ, Chubiz J, Raghuraman N, Zhao P, Tuuli MG, Wang L v, Cahill AG, Cuculich PS, Wang Y, Jungheim ES, et al. A multidisciplinary prematurity research cohort study. 2021: MedRxiv 2021 September 28.21264264.

Streeter GL, McMurrich JP, Keibel F, Mall FP. *The development of the nervous system*; 1912

Sydnor VJ, Larsen B, Bassett DS, Alexander-Bloch A, Fair DA, Liston C, Mackey AP, Milham MP, Pines A, Roalf DR, et al. Neurodevelopment of the association cortices: patterns, mechanisms, and implications for psychopathology. *Neuron*. 2021:109(18): 2820–2846.

Thomason ME, Marusak HA. Toward understanding the impact of trauma on the early developing human brain. *Neuroscience*. 2017:342:55–67.

Toulmin H, Beckmann CF, O'Muircheartaigh J, Ball G, Nongena P, Makropoulos A, Ederies A, Counsell SJ, Kennea N, Arichi T, et al. Specialization and integration of functional thalamocortical connectivity in the human infant. *Proc Natl Acad Sci*. 2015:112(20): 6485–6490.

Travis K, Ford K, Jacobs B. Regional dendritic variation in neonatal human cortex: a quantitative Golgi study. *Dev Neurosci*. 2005:27(5):277–287.

Turk E, van den Heuvel MI, Benders MJ, de Heus R, Franx A, Manning JH, Hect JL, Hernandez-Andrade E, Hassan SS, Romero R, et al. Functional connectome of the fetal brain. *J Neurosci*. 2019:39(49): 9716–9724.

Uddin, Lucina Q., B. T. Yeo, and R. Nathan Spreng. Towards a universal taxonomy of macro-scale functional human brain networks. *Brain topography*. 2019:32(6):926–942.

van Essen DC. A population-average, landmark- and surface-based (PALS) atlas of human cerebral cortex. *NeuroImage*. 2005:28(3): 635–662.

Varoquaux G, Raamana PR, Engemann DA, Hoyos-Idrobo A, Schwartz Y, Thirion B. Assessing and tuning brain decoders: cross-validation, caveats, and guidelines. *NeuroImage*. 2017:145(Pt B): 166–179.

Vogt BA, Watanabe H, Grootoonk S, Jones AK. Topography of diprenorphine binding in human cingulate gyrus and adjacent cortex derived from coregistered PET and MR images. *Hum Brain Mapp*. 1995:3(1):1–12.

Wakschlag LS, Roberts MY, Flynn RM, Smith JD, Krogh-Jespersen S, Kaat AJ, Gray L, Walkup J, Marino BS, Norton ES, et al. Future directions for early childhood prevention of mental disorders: a road map to mental health, earlier. *J Clin Child Adolesc Psychol*. 2019:48(3):539–554.

Warren DE, Power JD, Bruss J, Denburg NL, Waldron EJ, Sun H, Petersen SE, Tranel D. Network measures predict neuropsychological outcome after brain injury. *Proc Natl Acad Sci*. 2014:111(39): 14247–14252.

Werker JF, Tees RC. Speech perception as a window for understanding plasticity and commitment in language systems of the brain. *Dev Psychobiol*. 2005:46(3):233–251.